Epithelial-derived exosomes promote M2 macrophage polarization via Notch2/SOCS1 during mechanical ventilation

YANTING WANG[*], WANLI XIE[*], YIQI FENG, ZHENZHEN XU, YUYAO HE, YUE XIONG, LU CHEN, XIA LI, JIE LIU, GUOYANG LIU and QINGPING WU

Department of Anesthesiology, Union Hospital, Tongji Medical College,
Huazhong University of Science and Technology, Wuhan, Hubei 430022, P.R. China

Abstract. Alveolar macrophages (AMs) play an essential role in ventilator-induced lung injury (VILI). Exosomes and their cargo, including microRNAs (miRNAs/miRs) serve as regulators of the intercellular communications between macrophages and epithelial cells (ECs), and are involved in maintaining homeostasis in lung tissue. The present study found that exosomes released by ECs subjected to cyclic stretching promoted M2 macrophage polarization. It was demonstrated that miR-21a-5p, upregulated in epithelial-derived exosomes, increased the percentage of M2 macrophages by suppressing the expression of Notch2 and the suppressor of cytokine signaling 1 (SOCS1). The overexpression of Notch2 decreased the percentage of M2 macrophages. However, these effects were reversed by the downregulation of SOCS1. The percentage of M2 macrophages was increased in both short-term high- and low-tidal-volume mechanical ventilation, and the administration of exosomes-derived from cyclically stretched ECs had the same function. However, the administration of miR-21a-5p antagomir decreased M2 macrophage activation induced by cyclically stretched ECs or ventilation. Thus, the present study demonstrates that the intercellular transferring of exosomes from ECs to AMs promotes M2 macrophage polarization. Exosomes may prove to be a novel treatment for VILI.

Correspondence to: Professor Qingping Wu, Department of Anesthesiology, Union Hospital, Tongji Medical College, Huazhong University of Science and Technology, 1277 Jiefang Avenue, Wuhan, Hubei 430022, P.R. China
E-mail: wqp1968@126.com

[*]Contributed equally

Abbreviations: ALI, acute lung injury; AMs, alveolar macrophages; BALF, bronchoalveolar lavage fluid; BMDM, bone marrow-derived macrophage; BSA, bovine serum albumin; COPD, chronic obstructive pulmonary disease; CS, cyclic stretching; Co-IP, co-immunoprecipitation; DAPI, 4',6-diamidino-2-phenylindole; ECs, epithelial cells; GAPDH, glyceraldehyde 3-phosphate dehydrogenase; ELISA, enzyme-linked immunosorbent assay; KEGG, Kyoto Encyclopedia of Genes and Genomes; FACS, fluorescence-activated cell sorting; LDH, lactate dehydrogenase; LPS, lipopolysaccharide; PBS, phosphate-buffered saline; PMNs, polymorphonuclear neutrophils; RIPA, radioimmunoprecipitation assay; SOCS1, suppressor of cytokine signaling 1; VILI, ventilator-induced lung injury

Introduction

Mechanical ventilation is the main respiratory support provided for patients with lung injury or those under general anesthesia. However, ventilator-induced lung injury (VILI), involving inflammation, alveolar barrier disruption and hypertonic pulmonary edema, is a common complication. Pro-inflammatory factors (1-3) and macrophages (4) play a key role in VILI (5).

Alveolar macrophages (AMs) and alveolar epithelial cells (ECs) are the most critical cells for maintaining lung homeostasis (6,7). AMs are the major immune cells in lung tissue (8), suppressing inflammatory responses at homeostasis by releasing anti-inflammatory mediators, and play a crucial role in the inflammation progress in the lungs (9). Macrophages can be classified into pro-inflammatory M1 macrophages and anti-inflammatory M2 macrophages according to environmental stimuli (10). Alveolar ECs represent physical barrier that protects from external harmful substances. It has been demonstrated that the maintenance of homeostasis in the lungs is largely attributed to the interaction between ECs and macrophages (11). AMs adhere to ECs through CD200R, PD1 and their ligands CD200 and PDL1 on ECs. These protein interactions suppress the activation of AMs. In a steady state, ECs maintain macrophages in a quiescent state. In addition, ECs regulate the immune response and AM functions by secreting multiple mediators. Moreover, ECs participate in the recruitment and regulation of macrophages (12,13). ECs are also involved in mechanotransduction and the inflammatory response during mechanical ventilation (14,15). Thus, the interactions between AMs and ECs may serve as a novel therapeutic strategy for mechanical-induced lung injury.

The interactions between ECs and AMs include gap junctions (16), the secretion of molecules (17) and exosomes (7). Exosomes are small (20-200 nm in diameter) single-membrane

vesicles, which have been considered as a novel communication mechanism of intercellular due to transfer microRNAs (miRNAs/miRs), DNAs, lipids and proteins, and have various biological functions via autocrine and paracrine mechanisms (18). miRNAs are small non-coding RNAs that can induce the degradation or transcriptional repression of target genes (19). miRNAs play crucial roles in cell differentiation, proliferation, migration and apoptosis. Numerous studies have demonstrated that miRNAs play an essential role in lung diseases. miRNAs, such as miR-155, miR-26a, miR-21a-5p, miR-223, etc., have been shown to be involved in lung homeostasis and development (20). The inhibition of miR-221 has been found to ameliorate lipopolysaccharide (LPS)-induced lung injury (21), and miR-127 has been shown to be involved in VILI through the NF-κB and p38MAPK signaling pathways (22). Notably, miR-21a-5p, as one of the most crucial miRNAs, has been reported to be involved in the occurrence and development of various lung diseases (23,24), including asthma, chronic obstructive pulmonary disease (COPD) and acute lung injury (ALI). It has been demonstrated that miR-21a-5p negatively regulates the inflammatory response by interacting with immune cells in LPS-induced ALI (25). In addition, miR-21a-5p has been defined as a biomarker and therapeutic target (26). Exosomal miRNAs can mediate intercellular communications between several types of cells, which have been reported to influence biological pathways and further alter cellular functions (27). Exosomal miR-30d-5p-derived from polymorphonuclear neutrophil (PMN)-induced M1 macrophage polarization to promote sepsis-related ALI (28). Alveolar EC-derived exosomal miR-92a-3p has also been shown to activate macrophages by regulating the NF-kB signaling pathway and suppressing PTEN (29). However, the role of exosomes in the epithelial-macrophage interaction in mechanical ventilation has not yet been fully elucidated.

Considering the functions of exosomes, the present study, aimed to determine whether exosomes-derived from ECs subjected to cyclic stretching (CS) can regulate macrophage polarization. In addition, miRNA intervention was used to reveal the specific underlying mechanisms. The findings presented herein provide novel information on the effects of EC-derived exosomal miRNAs on the polarization of macrophages, which may be used as a potential therapeutic approach for lung injury during mechanical ventilation.

Materials and methods

Ethics approval. All procedures for the animal experiments were approved (approval no. 2406) by the Institutional Animal Care and Use Committee at Tongji Medical College, Huazhong University of Science and Technology (Wuhan, China).

Bone marrow-derived macrophage (BMDM) isolation. Male C57BL/6 mice (7 weeks old) were obtained from Vital River Laboratory Animal Technology. BMDMs were isolated from 7 male C57BL/6 mice (7 weeks old; weight, 21±2 g). In brief, mice were sacrificed using an overdose of 2% sodium pentobarbital (100 mg/kg) administred by intraperitoneal injection. Following sacrifice, the muscle was trimmed and the bone marrow cells were flushed from the bone shafts with Roswell Park Memorial Institute (RPMI)-1640 medium

(cat. no. 11875093; Gibco; Thermo Fisher Scientific, Inc.) and centrifuged (500 x g, 4°C, 5 min). Subsequently, 5 ml erythrocyte lysis buffer (cat. no. BL503A, Biosharp) were added, followed by 10 ml RPMI-1640 medium. The mixture was then centrifuged (500 x g, 4°C, 5 min). The cells were filtered through a 70-μm strainer and incubated at 37°C for 7 days in RPMI-1640 medium containing 10% fetal bovine serum (FBS, cat. no. 10100147; Gibco; Thermo Fisher Scientific, Inc.). The macrophages were incubated with macrophage colony-stimulating factor (10 ng/ml, cat. no. 416-ML-050, R&D Systems, Inc.) to activate the M0 macrophages. Half the medium was replaced every 2 days.

Cells and cell culture. Raw264.7 cells (mouse macrophages) were obtained from the American Type Culture Collection (ATCC). MLE-12 cells (mouse lung ECs) were obtained from the Department of Thoracic Surgery, Nanjing Medical University Affiliated Cancer Hospital, Cancer Institute of Jiangsu Province. The Raw264.7 cells were cultured in DMEM (cat. no. 11965092; Gibco; Thermo Fisher Scientific, Inc.) with 10% FBS and the MLE-12 were cultured in DMEM/F12 (cat. no. 11330032; Gibco; Thermo Fisher Scientific, Inc.) with 10% FBS. THP1 cells (human monocytes) were purchased from ATCC and cultured in RPMI-1640 with 10% FBS. All three types of cells were maintained at 37°C in a humidified incubator containing 5% CO_2.

CS of cells. MLE-12 cells were seeded onto fibronectin-coated (10 μg/cm^2) flexible silastic membranes (5.0x10^5 cells/well) with 10% exosome-depleted FBS (cat. no. AB-FBS-ED-0500, ABW GmbH), and divided into the following groups: i) The non-CS group (non-CS); ii) and the CS group. In the CS group, the cells were subjected to CS for 6 h, using the Flexercell Tension Plus TM FX-5000T system (Flexcell International) set at 20% elongation with 30 cycles/min as previously described (30).

Treatment of macrophages. BMDM or Raw264.7 macrophages were seeded in 6-well plates (5.0x10^5 cells/well), grown to 70-80% confluence, and divided into the following groups: i) The non-CS-exo (incubated with exosomes, which were isolated from non-CS group medium); and ii) the CS-exo group (incubated with exosomes isolated from CS group medium). The cells were treated with non-CS-exo or CS-exo (100 μg/ml), as previously described (28) for 12 h.

Cell transfection. Raw264.7 macrophages were transfected with miR-21a-5p mimic or negative control (NC) (100 nM, synthesized by Guangzhou RiboBio Co., Ltd.) using HiPerFect transfection reagent (cat. no. 301707; Qiagen GmbH). The miR-21a-5p mimic/NC sequences were: miR-21a-5p mimic sense, 5'-UAGCUUAUCAGACUGAUGUUGA-3' and anti-sense, 5'-UCAACAUCAGUCUGAUAAGCUA-3'; miR-21a-5p NC sense, 5'-UUUGUACUACACAAAAGU ACUG-3' and anti-sense, 5'-CAGUACUUUUGUGUAGUA CAAA-3'. Raw264.7 macrophages were also transfected with SOCS1 siRNA or NC (100 nM, synthesized by Guangzhou RiboBio Co., Ltd.) for 21 h and then treated with Jagged-1 (JAG; 20 ng/ml, cat. no. ab109346, Abcam) for 3 h. The SOCS1 siRNA/NC target sequences were: SOCS1 siRNA, 5'-CTA

CCTGAGTTCCTTCCCC-3'; SOCS1 NC, 5'-TTCTCCGAA CGTGTCACGT-3'. Raw264.7 macrophages were transfected with SOCS1 siRNA or NC at 37˚C for 24 h. The results of the cell transfection efficiency with miR-21a-5p mimic and SOCS1 siRNA are presented in Fig. S1A and B.

Raw264.7 were transfected with miR-21a-5p inhibitor or NC (100 nM, Guangzhou RiboBio Co., Ltd.) using HiPerFect transfection reagent (cat. no. 301707, Qiagen GmbH) 24 h before co-culturing with exosomes derived from ECs subjected to CS. Raw264.7 cells were transfected with miR-21a-5p inhibitor or NC at 37˚C for 24 h. The miR-21a-5p inhibitor/NC sequences were: miR-21a-5p inhibitor, 5'-UCAACAUCAGUCUGAUAA GCUA-3'; miR-21a-5p NC, 5'-CAGUACUUUUGUGUAGUA CAAA-3'. The cell transfection efficiency with miR-21a-5p inhibitor is presented in Fig. S1C.

MLE12 cells were seeded onto fibronectin-coated (10 μg/cm^2) flexible silastic membranes (5.0x10^5 cells/well) and transfected with fluorescein amidite (FAM)-miR-21a-5p mimic (100 nM, Guangzhou RiboBio Co., Ltd.) at 37˚C for 24 h. The cell transfection efficiency with FAM-miR-21a-5p mimic is presented in Fig. S2A. The cells were subjected to CS for 6 h as described above. The exosomes which contained FAM-miR-21a-5p mimic were isolated from the medium of MLE12 cells subjected to CS.

THP1 cells were seeded in 6-well plates (5.0x10^5 cells/well), and were differentiated from monocytes following treatment with phorbol 12-myristate 13-acetate (PMA, 100 nM, cat. no. P8139, MilliporeSigma) for 48 h. The THP1 cells were then transfected with miR-21a-5p mimic or NC (100 nM, Guangzhou RiboBio Co., Ltd.) using HiPerFect transfection reagent (cat. no. 301707; Qiagen GmbH) at 37˚C for 48 h. The cell transfection efficiency with miR-21a-5p mimic is presented in Fig. S2B.

Reverse transcription-quantitative PCR (RT-qPCR). Total RNA, including miRNA, was extracted from cultured cells, exosomes and lung tissues using RNAiso Plus (cat. no. 9109, Takara Bio, Inc.) according to the manufacturer's recommendations. The concentration of RNA was measured using a NanoDrop Lite UV-Vis spectrometer (ND-LITE, Thermo Fisher Scientific, Inc.). The PrimeScript™ RT kit (cat. no. RR037A, Takara Bio, Inc.) was used for miRNA and mRNA reverse transcription. A total of 500 ng RNA was used to synthesize the cDNA. miRNA and mRNA qPCR analyses were performed using TB Green® Premix Ex Taq™ II (cat. no. RR820A, Takara Bio, Inc.) and TB Green® Premix Ex Taq™ (cat. no. RR420A, Takara Bio, Inc.), respectively. The reactions were performed in triplicate at 95˚C for 30 sec, followed by 40 cycles at 95˚C for 15 sec, 60˚C for 30 sec; and 95˚C for 15 sec, 60˚C for 1 min, 95˚C for 15 sec on an ABI StepOne Real-Time PCR System, with U6 and glyceraldehyde 3-phosphate dehydrogenase (GAPDH) or β-actin used as the reference genes for miRNAs and mRNAs, respectively. GAPDH was used as a human reference gene and β-actin was used as a mouse reference gene. The mRNA primers (Tables SI and SII) were synthesized by TSINGKE Biological Technology, Co., Ltd. and miRNA primers (Table SI) were synthesized by Guangzhou RiboBio Co., Ltd. The relative expression levels were calculated using the 2$^{-\Delta\Delta Cq}$ method (31).

Exosome isolation, characterization and treatment. Exosomes were isolated from the medium of ECs in the CS or non-CS groups. To remove the cells, the medium was first centrifuged at 300 x g for 10 min, then centrifuged at 12,000 x g for 30 min to remove platelets and filtered using a 0.22 μm polyvinylidene fluoride (PVDF) filter (MilliporeSigma). The supernatant was then centrifuged at 120,000 x g with a Type 70 Ti (Beckman Coulter, Inc.) for 70 min to pellet the exosomes. All procedures for centrifugation were performed at 4˚C. The final pellet containing exosomes were resuspended in 200 μl phosphate-buffered saline (PBS, cat. no. BL302A, Biosharp) and stored at -80˚C for use in further experiments. The size distribution of exosomes was assessed using Nanosight tracking analysis (NTA).

Transmission electron microscopy (TEM). TEM was performed as previously described (32). Briefly, exosome pellets from medium from cells in the CS group were fixed with 2.5% glutaraldehyde at 4˚C for 30 min. A drop of exosome sample was placed on a carbon-coated copper grid for 10 min, followed by removal of excess exosomes with absorbent paper, immersion in 1% phosphotungstic acid solution (pH 7.0) for 30 sec, drying and examination using a JEOL JEM-1200EX (JEOL Ltd.) transmission electron microscope at an acceleration voltage of 80 kV.

Macrophage uptake of labelled exosomes. Exosomes or exosomes which contain FAM-miR-21a-5p mimic were labeled with PKH26 (cat. no. MINI26, MilliporeSigma). Subsequently, 100 μl exosome suspension were mixed with 500 μl Diluent C and 2 μl PKH26 to label the membranes. Following incubation for 5 min at room temperature, 1 ml of 1% bovine serum albumin (BSA, cat. no. BS114-100g, Biosharp) was added to terminate the labeling reaction. Thereafter, PKH-26-labeled exosomes (10 μg) were added to the Raw264.7 cells and incubated at 37˚C for 12 h. Nuclei were stained with 4',6-diamidino-2-phenylindole (DAPI, cat. no. F6057, MilliporeSigma) at room temperature for 5 min and viewed under a confocal microscope (Olympus Corporation).

Enzyme-linked immunosorbent assay (ELISA) of cytokines. The TNF-α, IL-1β, IL-6 and IL-10 levels in cell culture supernatants were assessed using TNF-α (cat. no. EMC102a.96), IL-1β (cat. no. EMC001b.96), IL-6 (cat. no. EMC004.96) and IL-10 (cat. no. EMC005.96) (all from Neobioscience Technology Co., Ltd.) ELISA kits following the manufacturer's protocols. The activity of lactate dehydrogenase (LDH) was detected using an LDH Activity Assay kit (cat. no. E-BC-K046-M, Elabscience Biotechnology, Inc.).

Cells in bronchoalveolar lavage fluid (BALF). A total of 279 male C57BL/6 mice (8 weeks old) were obtained from Vital River Laboratory Animal Technology. They were raised in a specific pathogen-free environment at 23±2˚C with a relative humidity of 40-60%, 12-h light/dark cycle. The mice were provided with free access to food and water.

A total of 63 male C57BL/6 mice (weight, 21±2 g) were randomly divided into three groups as follows: The control (ctrl), low-tidal-volume ventilation (LtVt, Vt=8 ml/kg) for 2 h,

and high-tidal-volume ventilation (HtVt, Vt=30 ml/kg) for 2 h. At the end of ventilation, the mice were sacrificed using an overdose of 2% sodium pentobarbital (100 mg/kg). The lungs were exposed and BALF was collected with 1.0 ml pre-cooled PBS (cat. no. BL302A, Biosharpa) through a tracheal cannula and repeated three times. BALF from 3 mice was collected into a 50 ml centrifuge tube and centrifuged at 1,000 x g for 5 min at 4℃ to collect cells and analyzed by flow cytometry. The lung tissues were collected for further analysis.

Exosome administration in vivo. To explore the function of exosome *in vivo*, a total of 51 male C57BL/6 mice were randomly divided into three groups as follows: The control (ctrl), non-CS-exo and CS-exo. The mice were administrated with non-CS-exo or CS-exo (300 μg/mouse) (28) through a tracheal cannula. After 24 h, the animals were sacrificed with an overdose of 2% sodium pentobarbital, and the lung tissues were then collected. The cells in BALF were collected according to the methods described above and analyzed using a LSRFortessa flow cytometer (BD Biosciences).

A total of 60 male C57BL/6 mice were randomly divided into two groups as follows: The CS-exo + NC and CS-exo + anti-miR-21a-5p groups. For miR-21a-5p inhibition, the miR-21a-5p antagomir (Guangzhou RiboBio Co., Ltd.) were used according to the manufacturer's instructions. Briefly, the mice were administered miR-21a-5p antagomir or NC (2.5 nM/mouse) 24 h prior to the challenged with CS-exo (300 μg/mouse) through a tracheal cannula.

Animal treatment. A total of 45 male C57BL/6 mice were randomly divided into five groups as follows: The ctrl + NC, LtVt + NC, LtVt + anti-miR-21a-5p, HtVt + NC and HtVt + anti-miR-21a-5p groups. The mice were administered miR-21a-5p antagomir or NC (2.5 nM/mouse) 24 h prior to the administration of LtVt or HtVt. Following ventilation for 2 h, the mice were sacrificed using an overdose of 2% sodium pentobarbital (100 mg/kg) and the cells in BALF were collected according to the methods described above.

A total of 60 male C57BL/6 mice were randomly divided into four groups as follows: The PBS + NC, JAG + NC, PBS + miR-21a-5p agomir and JAG + miR-21a-5p agomir groups. The miR-21a-5p agomir or NC (Guangzhou RiboBio Corporation, China) were used according to the manufacture's instruction. Mice were administrated with miR-21a-5p agomir or NC (2.5 nM/mouse) 24 h and sacrificed with an overdose of 2% sodium pentobarbital, then collected the lung tissues and the cells in BALF according to the methods described above. The miR-21a-5p agomir or NC (Guangzhou RiboBio Co., Ltd.) and JAG were used according to the manufacturer's instructions. The mice were administered miR-21a-5p agomir or NC (2.5 nM/mouse) 23 h prior to the challenge with JAG (0.5 mg/kg) or PBS through a tracheal cannula. Following the challenge with JAG for 1 h, the mice were sacrificed as described above, and the BALF and lung tissues were collected for further analysis.

Dual-luciferase reporter assays. TargetScan (http://www.targetscan.org/vert_71/) assays were used to identify potential miR-21a-5p targets. In this website, the species 'mouse' was selected, the microRNA name 'miR-21-5p' was entered and

the 'submit' button was then clicked. Target genes were then screened according to 'Cumulative weighted context + + score' and 'Total context + + score'. 293T cells (obtained from ATCC) at 70-80% confluence was co-transfected with wild-type or mutant Notch2 3'-UTR (i.e., with a mutated binding site) luciferase plasmids (50 ng, pmiR-RB-m-Notch2-WT or pmiR-RB-m-Notch2-MUT, respectively; Guangzhou RiboBio Co., Ltd.) and miR-21a-5p mimic or NC (50 nM, Guangzhou RiboBio Co., Ltd.) using HiPerFect transfection reagent. The *Firefly* luciferase activity was employed as the reference. Following incubation for 48 h at 37℃, the cells were assessed using a Dual-Luciferase Reporter Assay System (Promega Corporation) with a Glomax96 spectrophotometer (Promega Corporation). The cell transfection efficiency with miR-21a-5p mimic is presented in Fig. S2C.

Western blot analysis. Proteins were extracted from lung tissues or cultured cells using radioimmunoprecipitation assay (RIPA) buffer (cat. no. P0013B, Beyotime Institute of Biotechnology) with protease inhibitors (1:50, cat. no. 04693159001, Roche Diagnostics) and phosphatase inhibitors (1:50, cat. no. 04906837001, Roche Diagnostics). Protein concentrations were measured with a bicinchoninic acid assay kit (cat. no. 23227, Thermo Fisher Scientific, Inc.). Subsequently, 20 μg proteins were subjected to gel electrophoresis using 10% SDS-PAGE and electrophoretically transferred onto a PVDF membrane, then blocked with 5% BSA (cat. no. BS114-100g, Biosharp) for 1 h at room temperature. The membranes were then incubated with primary antibodies overnight at 4℃: Notch2 (1:1,000, cat. no. 5732, Cell Signaling Technology, Inc.), SOCS1 (1:500, cat. no. sc-518028, Santa Cruz Biotechnology, Inc.), GAPDH (1:10,000, cat. no. AC002, ABclonal Biotech Co., Ltd.), CD9 (1:400, cat. no. sc-13118, Santa Cruz Biotechnology, Inc.), CD63 (1:500, cat. no. A19023, ABclonal Biotech Co., Ltd.), CD81 (1:400; cat. no. sc-166029, Santa Cruz Biotechnology, Inc.), inducible nitric oxide synthase (iNOS; 1:1,000, cat. no. A0312, ABclonal Biotech Co., Ltd.), TNF-α (1:2,000, cat. no. 60291-1-lg, ProteinTech Group, Inc.), IL-6 (1:1,000, cat. no. 21865-1-AP, ProteinTech Group, Inc.), IL-1β (1:1,000, cat. no. 66737-1-lg, ProteinTech Group, Inc.), arginase 1 (Arg1; 1:5,000, cat. no. 16001-1-AP, ProteinTech Group, Inc.), CD206 (1:1,000, cat. no. 18704-1-AP, ProteinTech Group, Inc.), IL-10 (1:500, cat. no. 60291-1-lg, ProteinTech Group, Inc.), or β-actin (1:10,000, cat. no. AC026, ABclonal Biotech Co., Ltd.) and then incubated with goat anti-rabbit IgG HRP (1:5,000, cat. no. BL010A, Biosharp) or goat anti-mouse IgG HRP (1:5,000, cat. no. BL008A, Biosharp) antibodies for 1 h at room temperature. Images were captured using the UVP EC3 imaging system (Analytik Jena US LLC Co., Ltd.) and analyzed using ImageJ v1.52v software (National Institutes of Health).

Co-immunoprecipitation (Co-IP). After the BMDMs were treated with non-CS-exo or CS-exo, Co-IP was performed. Briefly, cells were lysed in RIPA lysis buffer (cat. no. P0013B, Beyotime Institute of Biotechnology), with protease inhibitors (1:50, cat. no. 04693159001, Roche Diagnostics) and phosphatase inhibitors (1:50, cat. no. 04906837001, Roche Diagnostics) for 30 min on ice. Following centrifugation at 12,000 x g for 15 min 4℃, the 1/10 volume of protein sample was isolated

as input, and half of the protein sample was incubated with 20 μl/ml protein A/G-beads (cat. no. 1614813, Bio-Rad Laboratories, Inc.) at 4˚C for 30 min. Following centrifugation at 12,000 x g for 15 min 4˚C, 1 μg Notch2 antibody or rabbit control IgG (cat. no. AC005, ABclonal Biotech Co., Ltd.) was co-incubated with the remaining sample at 4˚C for 1 h with gentle rotation. Subsequently, 20 μl beads were added and incubated overnight at 4˚C and the beads were then extracted and washed three times using RIPA buffer, and the bound proteins were boiled in 2X Laemmli buffer (cat. no. 1610737, Bio-Rad Laboratories, Inc.). Finally, the purified proteins were examined using western blot analysis.

Immunofluorescence. Raw264.7 macrophages were treated with non-CS-exo or CS-exo, washed twice with pre-cooled PBS, and fixed with 4% paraformaldehyde at 4˚C for 30 min. After blocking with 5% BSA (cat. no. BS114-100g, Biosharp) at room temperature for 1 h, the cells were incubated with SOCS1 (1:100, cat. no. sc-518028, Santa Cruz Biotechnology, Inc.) and Notch2 (1:100, cat. no. 5732, Cell Signaling Technology, Inc.) antibodies overnight at 4˚C, followed by incubation with Dylight 549, goat anti-rabbit IgG (1:200, cat. no. A23320, Abbkine Scientific Co., Ltd.) and DyLight 488, goat anti-mouse IgG (1:200, cat. no. A23210, Abbkine Scientific Co., Ltd.) at room temperature for 1 h on a horizontal shaker. Nuclei were stained with DAPI at room temperature for 5 min and images were captured using a fluorescence microscope (magnification, x400, Olympus Corporation).

mRNA library construction and sequencing. The MGISEQ2000 platform (BGI-Shenzhen) was applied to sequence the final ligation PCR products. i) RNA extraction: RNA was extracted from BMDMs treated with non-CS-exo or CS-exo using an RNeasy Mini kit (cat. no. 74104, Qiagen GmbH) according to the manufacturer's protocols, and 1.3 μg/sample total RNA was used for the construction of the sequencing libraries. Subsequently, total RNA was qualified and quantified using a Nano Drop and Agilent 2100 bioanalyzer (Thermo Fisher Scientific, Inc.). ii) mRNA library construction: mRNA molecules were purified with oligo (dT)-attached magnetic beads. The resulting mRNAs were cut into small sections with fragmentation reagent. First-strand cDNA was generated using random hexamer-primed reverse transcription, followed by a second-strand cDNA synthesis. The synthesized cDNA was subjected to end-repair and then was 3' adenylated. Adapters were ligated to the ends of these 3' adenylated cDNA fragments, and the cDNA fragments were then amplified and products were purified with Ampure XP Beads (Agencourt, cat. no. A63882, Beckman Coulter, Inc.), and dissolved in EB solution. For quality control, the library was validated on an Agilent Technologies 2100 bioanalyzer. Following heat denaturation, the double-stranded PCR products were circularized with the splint oligo sequence. The single-strand circle DNA (ssCir DNA) were formatted as the final library. The library was amplified with phi29 to yield DNA nanoball (DNB) with a molecular copy number >300. The DNBs were load into the patterned nanoarray, and the method of combinatorial Probe-Anchor Synthesis (cPAS) was used to generated single end 50 (pair end 100/150) bases reads. iii) Bioinformatics workflow: Bioinformatics was completed at BGI-Shenzhen. The detailed protocols were provided and demonstrated at the BGI website: http://www.bgitechsolutions.com/). The sequencing data were filtered with SOAPnuke (v1.5.2) as follows: a) Reads containing sequencing adapter were removed; b) reads with low-quality base ratio (base quality ≤5) >20% were removed; c) reads with an unknown base ('N' base) ratio >5% were removed, and clean reads were then obtained and stored in FASTQ format. The clean reads were mapped to the reference genome using HISAT2 (v2.0.4) and aligned to the reference coding gene set using Bowtie2 (v2.2.5), and RSEM (v1.2.12) was then used to calculate the expression levels of genes. Essentially, differential expression analysis was performed using the DESeq2 (v1.4.5) with a Q value ≤0.05. Pheatmap (v1.0.8) was used to draw the heatmap according to the expression of gene in different samples. The obtained novel genes have been deposited in the NCBI Gene Expression Omnibus Archive (accession no. GSE200932). Kyoto Encyclopedia of Genes and Genomes (KEGG) (https://www.kegg.jp/) enrichment analysis of annotated differentially expressed genes was performed.

Flow cytometry. Cells in BALF, Raw264.7 or BMDMs were passed through a 100-μm cell strainer, resuspended in fluorescence-activated cell sorting (FACS) buffer (0.5% FBS and 1 ml of 2 mM EDTA in PBS), followed by Fc Block (0.5 μg/ml, cat. no. 553141, BD Biosciences) at room temperature for 10 min. The cells were then stained with the following antibodies for 30 min: Fixable Viability Stain 510 (1:200, cat. no. 564406, BD Biosciences), APC-Cy7 CD45 (1:200, cat. no. 561037, BD Biosciences), V450 anti-CD11b (1:200, cat. no. 560456, BD Biosciences), phycoerythrin (PE) anti-F4/80 (1:400, cat. no. 565410, BD Biosciences), BB700 anti-CD11c (1:200, cat. no. 566505, BD Biosciences) and Alexa Fluor® 647 anti-CD206 (1:100, cat. no. 565250, BD Biosciences). The cells were incubated with antibodies at 4˚C in the dark and then analyzed using a BD LSRFortessa flow cytometer. Data were analyzed using FlowJo software (v10, TreeStar, Inc.).

Statistical analysis. Data are presented as the mean ± standard error of the mean (SEM). Means were compared between two groups using a two-tailed unpaired Student's t-test. One-way analysis of variance (ANOVA) was used among multiple groups followed by Tukey's post hoc test. The expression of mRNAs or miRNAs was log-transformed. $P<0.05$ was considered to indicate a statistically significant difference. All calculations were performed using GraphPad Prism 7.0 software (GraphPad Software, Inc.).

Results

Exosomes-derived from CS-treated ECs transferred miR-21a-5p to macrophages. Alveolar ECs are involved in mechanotransduction during mechanical ventilation (15). Thus, the present study subjected MLE-12 cells to CS for 0 and 6 h. No marked differences were observed in the levels of TNF-α, IL-6, IL-1β and LDH (Fig. S3). However, CS increased miR-21a-5p expression in MLE-12 cells (Fig. S4). Thus, CS did not result in significant changes in ECs, apart from the increase in miR-21a-5p expression in ECs.
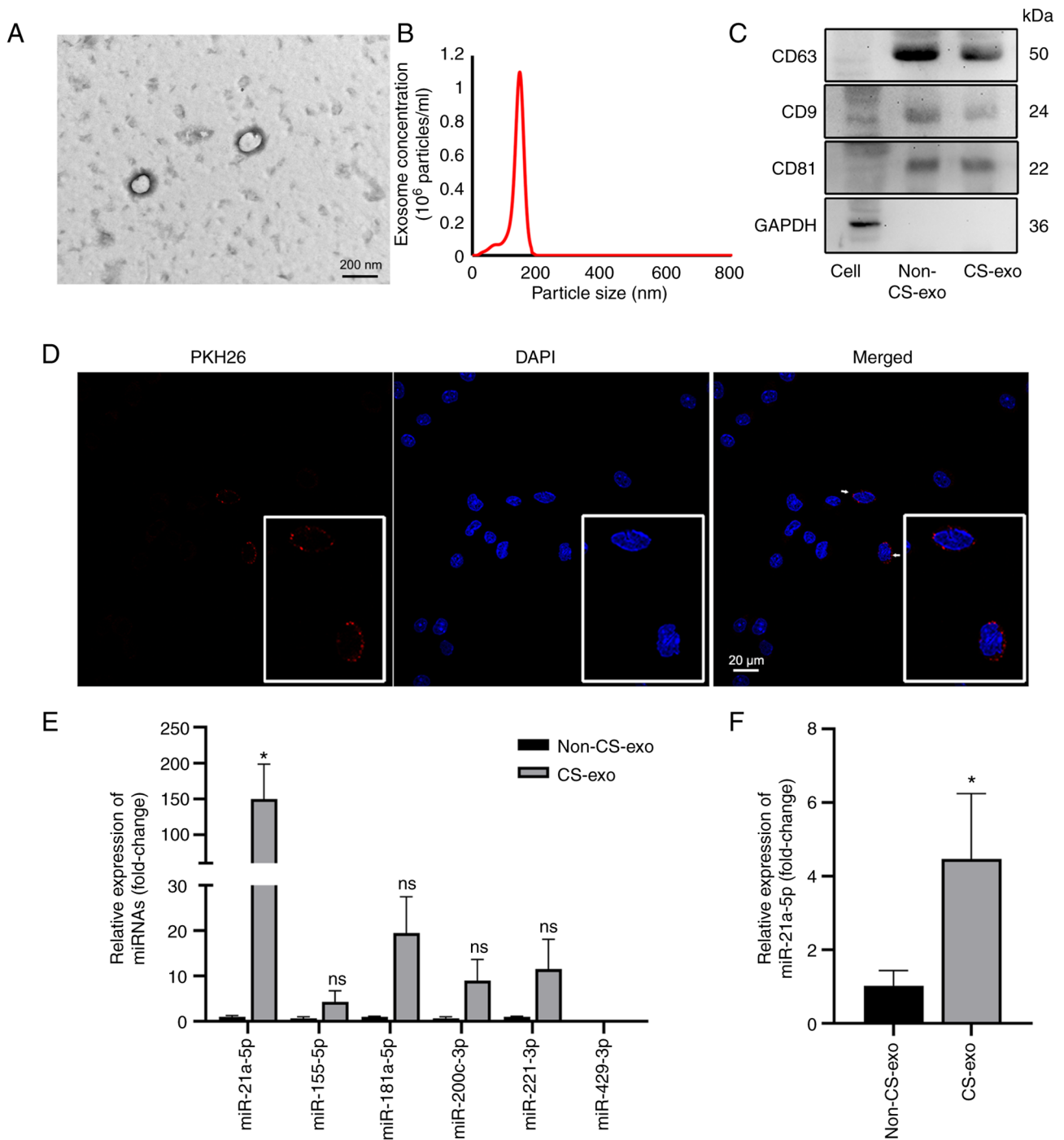
Figure 1. Exosomes from MLE-12 cells subjected to CS transfer miR-21a-5p to macrophages. (A) Electron microscopy images of exosomes isolated from medium of cells subjected to CS. Scale bar, 200 nm. (B) Particle size distribution, assessed using dynamic light scattering. (C) The levels of the exosomal markers, CD9, CD63 and CD81, and the internal reference, GAPDH, were assessed using western blot analysis. (D) Immunofluorescence images of macrophages incubated with PKH26-labeled exosomes (red) for 12 h. Nuclei was counterstained with DAPI (blue). Scale bar, 20 μm. (E) The expression levels of miRNAs in exosomes were assessed using reverse transcription-quantitative PCR (n=3). (F) The levels of miR-21a-5p in macrophages following treatment with exosomes (n=4). Data are expressed as the mean ± SEM. *P<0.05, vs. non-CS-exo group. CS, cyclic stretching; non-CS-exo, incubated with exosomes isolated from medium of cells not subjected to CS; CS-exo, incubated with exosomes isolated from medium of cells subjected to CS.

As inflammatory cytokine levels were not significantly altered by subjecting the MLE-12 cells to CS, the medium of MLE-12 cells was collected after CS, and exosomes were isolated (Fig. 1A-C) and then labeled with PKH26. The labeled exosomes were engulfed by macrophages following incubation with macrophages for 12 h (Fig. 1D). Exosomal miR-21a-5p expression (contained within the exosomes) was also increased in the exosomes derived from CS-exo compared with non-CS group cells (Fig. 1E). miR-21a-5p was particularly upregulated compared to other miRNAs related to lung injury, such as miR-155-5p (33), miR-181a-5p (34), miR-200c-3p (35), miR-221-3p (21), miR-429-3p (36) (Fig. 1E). In addition, the levels of miR-21a-5p in macrophages was increased in the CS-exo group compared with the non-CS-exo group (Fig. 1F).

To verify whether exosomal miR-21a-5p could be taken up by macrophages, macrophages were cultured with PKH26-labeled exosomes-derived from ECs transfected with FAM-miR-21a-5p mimic prior to CS, and FAM-miR-21a-5p signals (green) were detected in the macrophages' cytoplasm, colocalizing with PKH26 (red) (Fig. S5). These results demonstrated that ECs treated with CS could secrete exosomes carrying high levels of miR-21a-5p, and transfer this to macrophages.

Exosomes from CS-treated ECs promote M2 polarization. M1 macrophages have been implicated in several inflammatory conditions (37), while M2 macrophages exhibit anti-inflammatory or reparative functions (38,39). Distinct macrophage phenotypes contribute to lung inflammation or resolution (40). In the present study, CS did not induce notable changes in MLE-12 cells apart from the increase in miR-21a-5p expression. Exosomes were derived from CS-treated ECs (CS-exo) containing high levels miR-21a-5p, and the present study then determined whether 12 h of incubation with CS-exo induced macrophage inflammation in BMDMs. No marked differences were observed in the levels of IL-6 or TNF-α in the exosome-treated BMDMs (Fig. 2A); however, the levels of IL-10 increased in the CS-exo group compared with the non-CS-exo group (Fig. 2A). Flow cytometry revealed that the percentage of M2 macrophages (CD206+CD11c-) increased, while that of M1 macrophages (CD11c+CD206-) decreased in the CS-exo group (Fig. 2B and C). The levels of M1 and M2 macrophage markers detected using RT-qPCR (Fig. 2D and E) were basically consistent with the flow cytometry results. In addition, the protein expression levels of M1 macrophage-related markers (iNOS, TNF-α, IL-6 and IL-1β) and M2 macrophage-related markers (Arg1, CD206 and IL-10) in BMDMs in the non-CS-exo and CS-exo groups were examined using western blot analysis. The protein expression levels of iNOS, TNF-α, IL-6 and IL-1β were decreased in the CS-exo group compared with the non-CS-group, while the expression levels of Arg1, CD206 and IL-10 were increased in the CS-exo group (Fig. 2F-H). CS-exo also increased the M2 macrophage polarization of Raw264.7 cells compared to non-CS-exo (Fig. 2I and J). However, the percentage of M2 macrophages decreased following the inhibition of miR-21a-5p prior to co-culturing with exosomes, while the percentage of M1 macrophages increased (Fig. 2K and L). These data indicated that CS-treated EC-derived exosomal miR-21a-5p promoted M2 macrophage polarization.

Exosomal miR-21a-5p from CS-treated ECs targets Notch2 to regulate macrophage polarization. To determine the exact mechanisms by which miR-21a-5p induced macrophage polarization, TargetScan (http://www.targetscan.org/vert_71/) assays were used to identify potential miR-21a-5p targets, which led to the identification of Notch2. As the dual-luciferase reporter assays revealed, when wild-type Notch2 3'-UTR was used with the plasmid, miR-21a-5p overexpression decreased the relative luciferase activity (Fig. 3A); however, no significant change was observed when the miR-21a-5p binding site in the Notch2 3'-UTR was mutated. Moreover, miR-21a-5p mimic downregulated the expression of Notch2 in Raw264.7 macrophages at 24 h following transfection (Fig. 3B and C).

Furthermore, exosomes from the medium of CS-treated ECs also downregulated the expression of Notch2 mRNA (Fig. 3D) and protein (Fig. 3E and F) in macrophages. However, miR-21a-5p inhibition prior to co-culture with exosomes increased the protein expression of Notch2 (Fig. 3G and H).

The present study then activated Notch2 using its ligand, JAG (20 ng/ml), for 3 h (Fig. 3I and J). Flow cytometry revealed that the proportion of M2 macrophages was decreased in the Notch2 activation (JAG treatment) group (Fig. 3K and L). RT-qPCR was used to detect M1 and M2 markers; Arg1 and CD206 (M2 macrophage markers) mRNA expression was decreased, while iNOS, TNF-α, and IL-1β mRNA expression was increased (Fig. 3M and N). Thus, Notch2 was shown to be involved in macrophage polarization.

Notch2/SOCS1 axis regulates macrophage polarization. The Notch2 intracellular domain is transported to the nucleus, and then regulates the transcription of target genes (41). In the present study, to explore the downstream mechanisms of Notch2 during mechanical ventilation, the BMDMs in the non-CS-exo and CS-exo groups were subjected to RNA-seq. The genes associated with M2 macrophage polarization are presented in Fig. 4A. KEGG analysis revealed that these genes were enriched in signal transduction (Fig. 4B). Co-IP assays revealed that Notch2 interacted with SOCS1 in macrophages (Fig. 5A). Following treatment with non-CS-exo or CS-exo, SOCS1 mRNA expression (assessed using RT-qPCR) in macrophages was increased (Fig. 5B) in the CS-exo group compared with the non-CS-exo group, as in the RNA-seq analysis. SOCS1 protein expression (assessed using western blot analysis) was downregulated in macrophages (Fig. 5C and D). There are numerous complex and varied post-transcriptional mechanisms involved in turning mRNA into protein that are not yet sufficiently well-defined to be able to compute protein concentrations from mRNA (42); this may be the reason for the poor concordance between the level of SOCS1 mRNA and protein. The inhibition of miR-21a-5p also increased SOCS1 expression that was downregulated by CS-exo (Fig. 5E and F). The results of immunofluorescence staining revealed that CS-exo also reduced the fluorescence intensity of Notch2 and SOCS1 (Fig. 5G). As Notch2 activation (using JAG) decreased the percentage of M2 macrophages compared to the control group (Fig. 3K and L), the present study then verified the regulation of macrophage polarization by Notch2/SOCS1. Raw264.7 macrophages were transfected with SOCS1 siRNA or NC prior to JAG treatment. The percentage of M2 macrophages was increased in the siRNA group compared to the NC group (Fig. 5H and I). Thus, the Notch2/SOCS1 axis is involved in the M2 polarization of macrophages.

THP1 cells were also transfected with miR-21a-5p mimic to determine whether the miR-21a-5p/Notch2/SOCS1 axis regulates macrophage polarization in human cells. The expression levels of Notch2 and SOCS1 (Fig. S6A-C) were suppressed following transfection with miR-21a-5p mimic. The results of RT-qPCR also revealed that the levels of M1 macrophage markers were downregulated and those of M2 macrophage markers were upregulated (Fig. S6D and E). These results further confirmed that the miR-21a-5p/Notch2/SOCS1 axis regulated macrophage polarization.
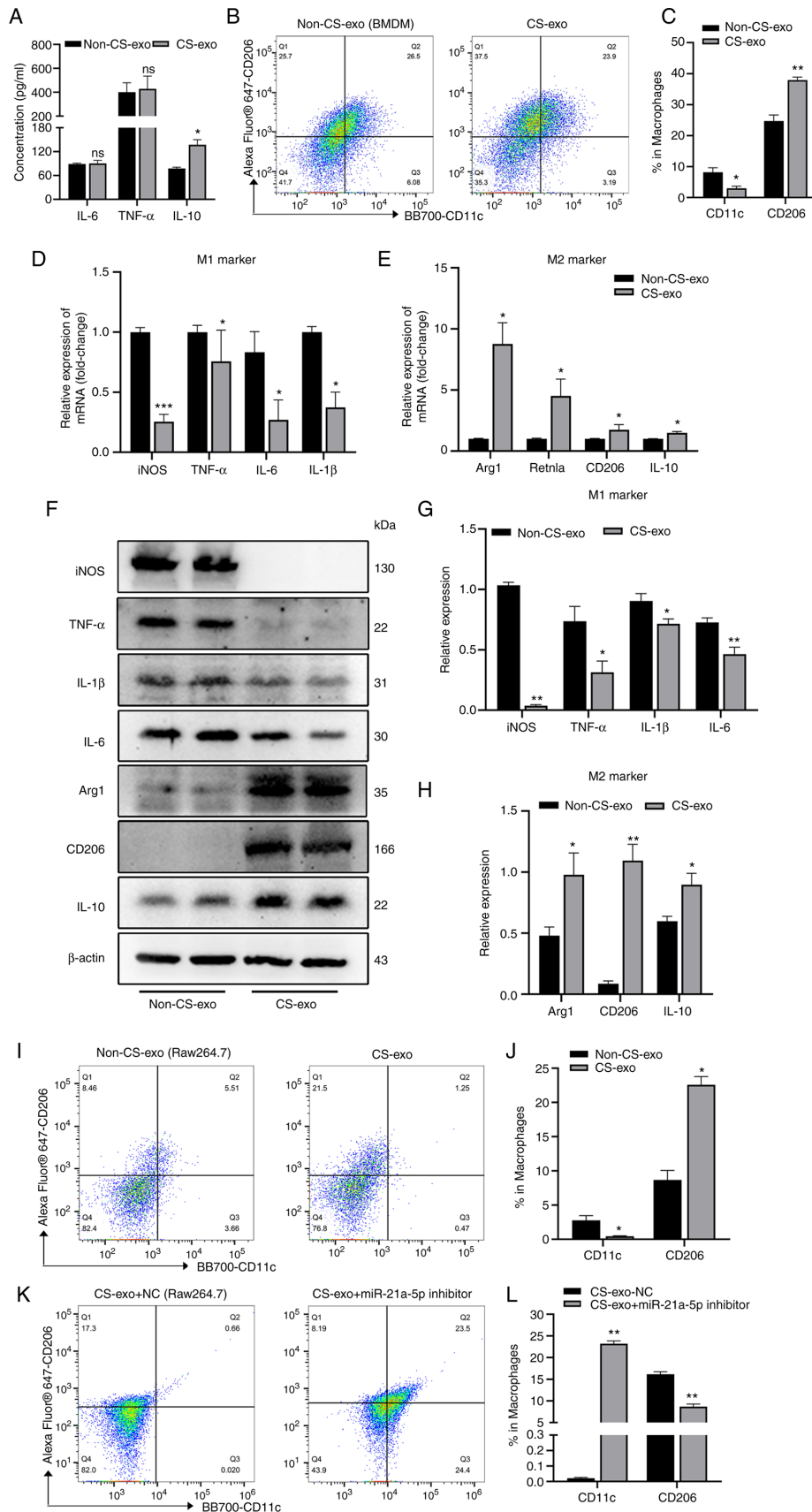
Figure 2. CS-exo promotes the M2 polarization of macrophages. Exosomes derived from MLE-12 cells subjected to CS for 6 h were added to BMDMs or Raw264.7 macrophages for 12 h. (A) IL-6, TNF-α and IL-10 levels in supernatant of BMDMs, assessed using ELISA (n=4). (B and C) Measurement of the expression of CD11c and CD206 on BMDMs, assessed using flow cytometry (n=4). (D and E) Macrophage markers, assessed using reverse transcription-quantitative PCR (n=7). (F-H) Protein expression levels of iNOS, TNF-α, IL-1β, IL-6, Arg1, CD206 and IL-10 in BMDMs following treatment with exosomes (n=4). (I and J) Measurement of the expression of CD11c and CD206 in Raw264.7 cells (n=3). (K and L) Inhibition of miR-21a-5p (using miR-21a-5p inhibitor) prior to CS-exo. Flow cytometry was used to detect CD11c and CD206 expression (n=3). Data are expressed as the mean ± SEM. $^{*}P<0.05$, $^{**}P<0.001$ and $^{***}P<0.001$, vs. non-CS-exo group. ns, not significant; CS, cyclic stretching; non-CS-exo, incubated with exosomes isolated from medium of cells not subjected to CS; CS-exo, incubated with exosomes isolated from medium of cells subjected to CS; BMDM, bone marrow-derived macrophage; iNOS, inducible nitric oxide synthase; Arg1, arginase 1.
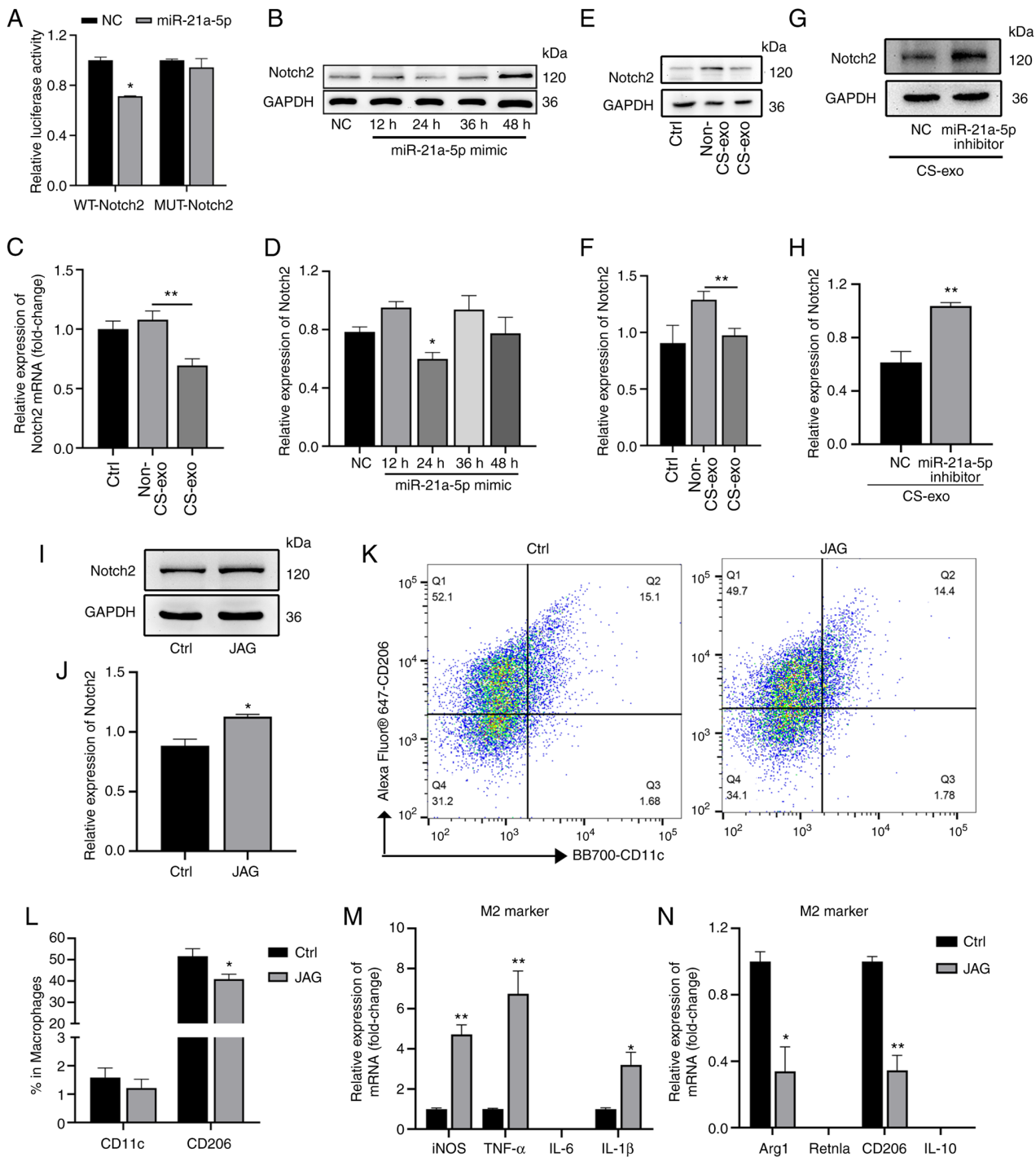
Figure 3. Exosomal miR-21a-5p derived from epithelial cells subjected to CS targets Notch2 in macrophages. (A) Luciferase reporter assay following co-transfection with miR-21a-5p mimic or NC and wild-type or mutant Notch2 3'-UTR luciferase plasmid (50 ng) (n=3). (B and C) Notch2 expression in Raw264.7 macrophages treated with miR-21a-5p mimic for 12, 24, 36 and 48 h, assessed using western blot analysis (n=3). (D) Raw264.7 cells were treated with exosomes and Notch2 mRNA expression was assessed using RT-qPCR (n=5). (E and F) Raw264.7 cells were treated with exosomes and Notch2 protein expression was assessed using western blot analysis (n=6). (G and H) Raw264.7 cells were treated with miR-21a-5p inhibitor prior to CS-exo treatment. Western blot analysis was used to detect the expression of Notch2 (n=3). (I and J) Notch2 protein expression in Raw264.7 macrophages was assessed using western blot analysis following treatment with JAG for 3 h (n=3). (K and L) Proportions of M1 and M2 macrophages (determined using anti-CD11c and anti-CD206 antibodies, respectively) following treatment with 20 ng/ml JAG for 3 h, assessed using flow cytometry (n=7). (M and N) Macrophage markers following treatment with 20 ng/ml JAG for 3 h, assessed using RT-qPCR (n=3). Data are expressed as the mean ± SEM. *P<0.05 and **P<0.001, vs. the respective control. ctrl, control; NC, negative control; JAG, Jagged-1; WT, wild-type; MUT, mutant; RT-qPCR, reverse transcription-quantitative PCR; CS, cyclic stretching; non-CS-exo, incubated with exosomes isolated from medium of cells not subjected to CS; CS-exo, incubated with exosomes isolated from medium of cells subjected to CS; iNOS, inducible nitric oxide synthase; Arg1, arginase 1; Retnla, resistin like alpha.

miR-21a-5p regulates mechanical ventilation-induced M2 polarization through Notch2/SOCS1 in vivo. The present study then verified the function of epithelial-derived exosomal miR-21a-5p *in vivo.* The administration of CS-exo significantly increased the expression of miR-21a-5p in mouse lung tissues (Fig. 6A). Following treatment with CS-exo, the iNOS, TNF-α
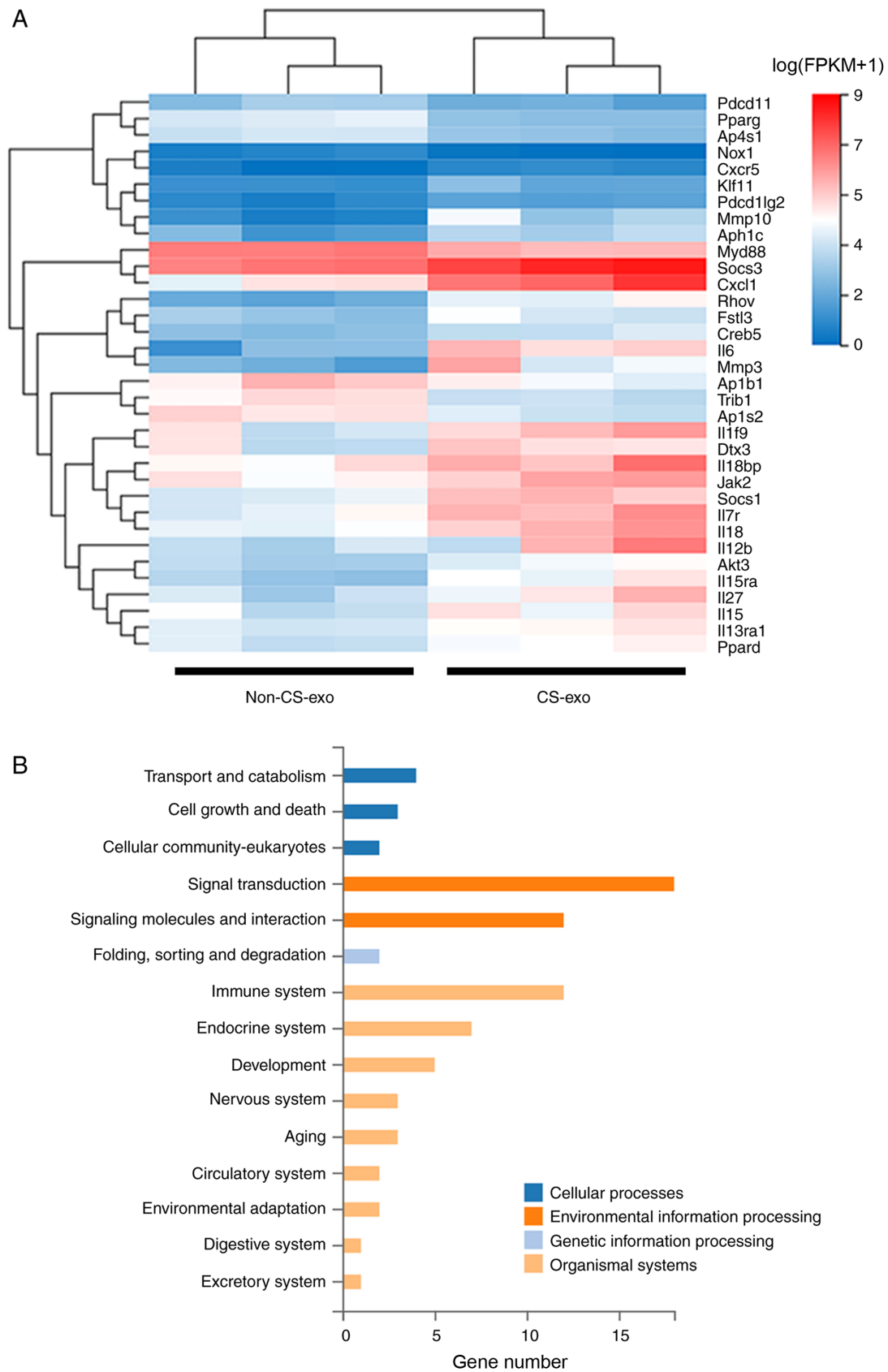
Figure 4. Differential mRNA expression and functional analysis. (A) Heatmap of genes related to macrophage polarization after exosomes from the CS or non-CS group were added to macrophages, assessed using RNA-seq. (B) Kyoto Encyclopedia of Genes and Genomes pathway analysis.

and IL-1β mRNA (M1 macrophage markers) expression levels were decreased (Fig. 6B), while those of Arg1, resistin like alpha (Retnla), CD206 and IL-10 mRNA (M2 macrophage markers) were increased (Fig. 6C). CS-exo also increased the proportion of M2 macrophages, and decreased the proportion of M1 macrophages in BALF (Fig. 6D and E). Moreover,
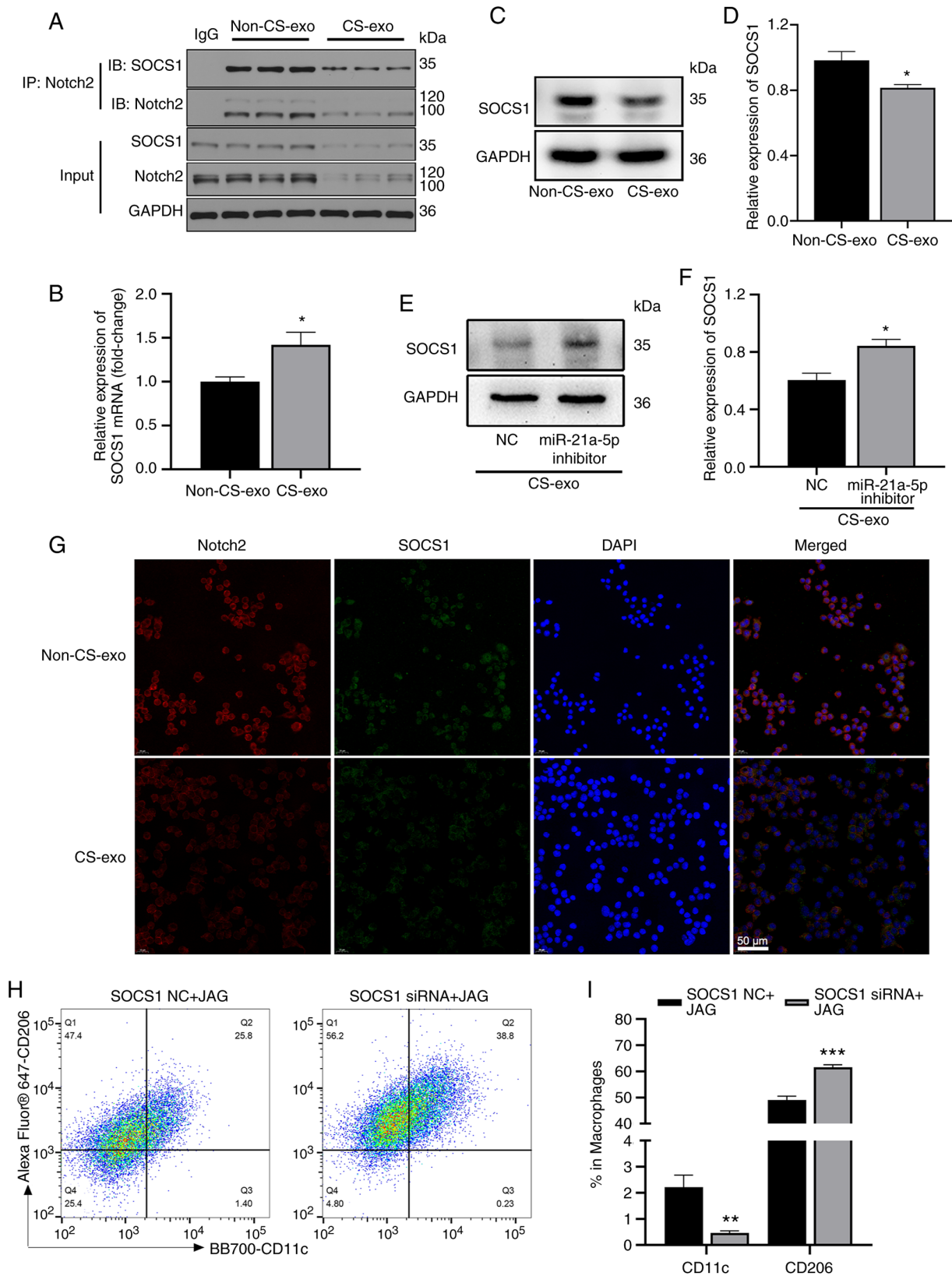
Figure 5. The Notch2/SOCS1 axis regulates macrophage polarization. (A) Bone marrow-derived macrophages in the non-CS-exo and CS-exo groups were immunoprecipitated with anti-Notch2 antibody, or rabbit control IgG, and the precipitates were examined using western blot analysis [immunoblotting (IB)] with anti-Notch2 or anti-SOCS1 antibodies (n=3). (B) SOCS1 mRNA expression in macrophages following treatment with exosomes (n=6). (C and D) SOCS1 protein expression in macrophages following treatment with exosomes (n=3). (E and F) Raw264.7 cells were transfected with miR-21a-5p inhibitor or NC prior to CS-exo treatment. SOCS1 expression in macrophages was detected using western blot analysis (n=3). (G) Immunofluorescence co-staining of SOCS1 and Notch2 in Raw264.7 macrophages following treatment with exosomes (n=3). (H and I) Proportions of M1 and M2 macrophages (determined using anti-CD11c and anti-CD206 antibodies, respectively) following treatment with SOCS1 siRNA or NC prior to JAG treatment, assessed using flow cytometry (n=6). Data are expressed as the mean ± SEM. *P<0.05, vs. non-CS-exo group; **P<0.001 and ***P<0.0001, vs. NC. NC, negative control; JAG, Jagged-1; CS, cyclic stretching; non-CS-exo, incubated with exosomes isolated from medium of cells not subjected to CS; CS-exo, incubated with exosomes isolated from medium of cells subjected to CS; SOCS1, suppressor of cytokine signaling 1.
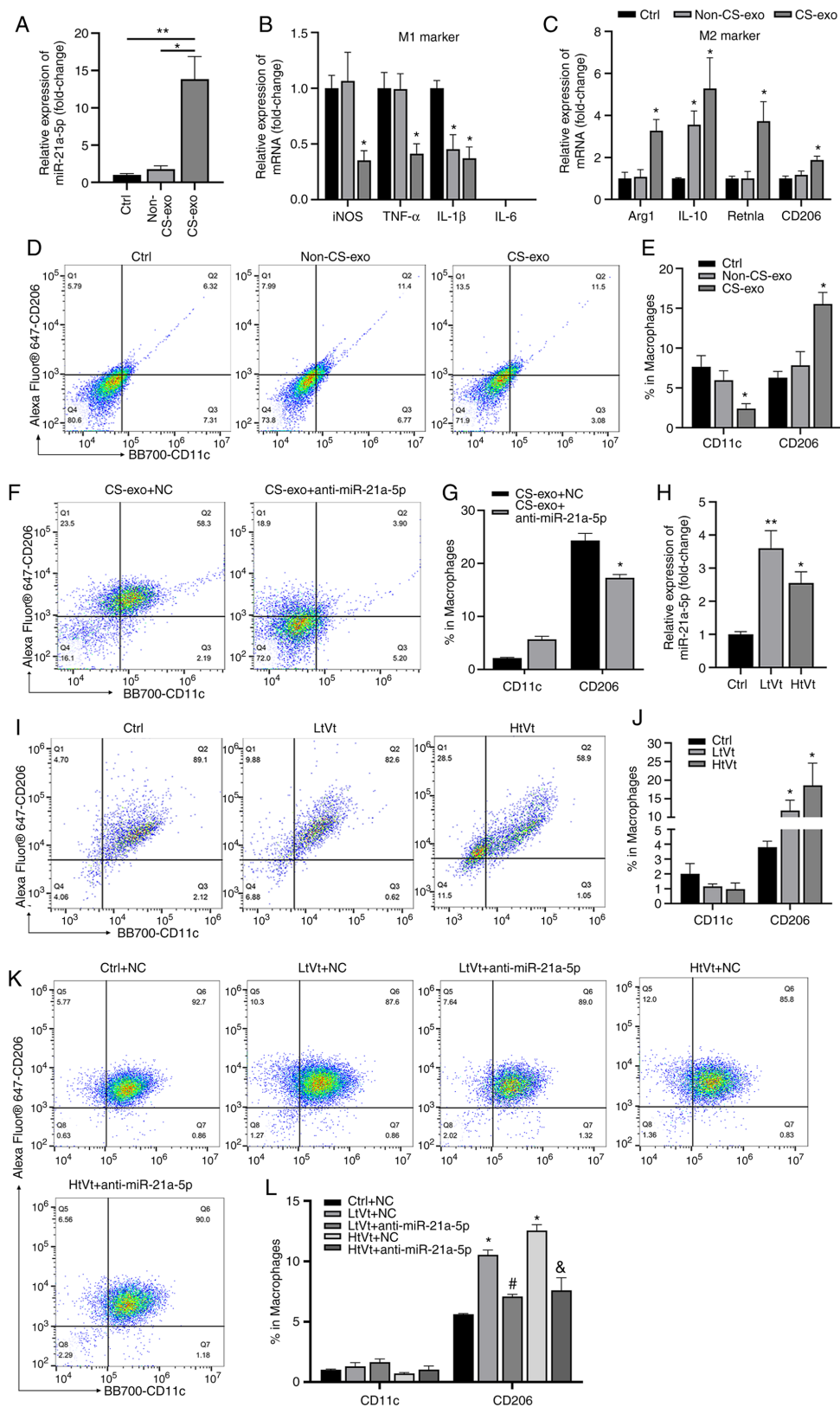
Figure 6. miR-21a-5p regulates M2 polarization induced by mechanical ventilation *in vivo*. Mice were challenged CS-exo through a tracheal cannula or subjected to mechanical ventilation. Mice were administered miR-21a-5p antagomir or NC 24 h prior to treatment with CS-exo or mechanical ventilation. (A) Mice were treated with CS-exo, and the level of miR-21a-5p in lung tissue was assessed using RT-qPCR (n=8). (B and C) Macrophage markers, assessed using RT-qPCR (n=6). (D and E) The expression of CD11c and CD206 in cells in BALF was measured using flow cytometry (n=9). (F and G) Mice were administered miR-21a-5p antagomir or NC 24 h prior to treatment with CS-exo. The expression of CD11c and CD206 in cells in BALF was detected using flow cytometry (n=9). (H) The expression of miR-21a-5p in lung tissues of mice subjected to LtVt or HtVt or the ctrl procedure for 2 h was assessed using RT-qPCR (n=8). (I and J) Macrophage phenotypes in BALF of mice subjected to LtVt or HtVt or the ctrl procedure for 2 h were assessed using flow cytometry (n=12). (K and L) The expression of CD11c and CD206 in cells in BALF was detected using flow cytometry (n=9). Data are expressed as the mean ± SEM. *P<0.05 and **P<0.01, vs. control; #P<0.05, vs. LtVt + NC; &P<0.05, vs. HtVt + NC. NC, negative control; CS, cyclic stretching; non-CS-exo, incubated with exosomes isolated from medium of cells not subjected to CS; CS-exo, incubated with exosomes isolated from medium of cells subjected to CS; RT-qPCR, reverse transcription-quantitative PCR; BALF, bronchoalveolar lavage fluid; Arg1, arginase 1; Retnla, resistin like alpha; LtVt, low-tidal-volume ventilation; HtVt, high-tidal-volume ventilation.
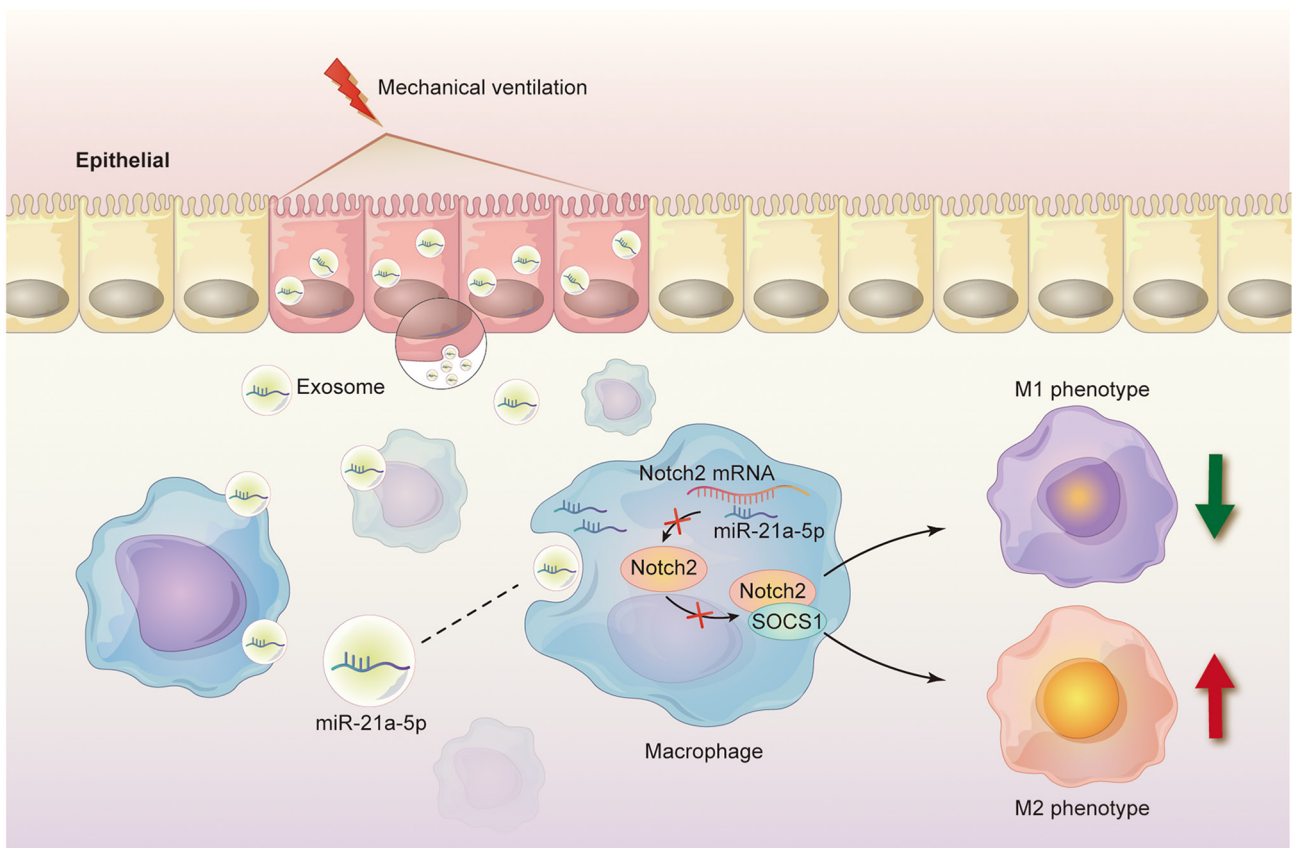
Figure 7. Schematic diagram of the mechanisms underlying the protective anti-inflammatory effects of mechanical ventilation. Epithelial cells secrete exosomes containing miR-21a-5p, which are engulfed by macrophages. miR-21a-5p represses Notch2, which downregulates SOCS1, promoting M2 macrophage polarization. Thus, the communication between epithelial cells and macrophages involving exosomal miR-21a-5p exerts a protective effect during mechanical ventilation. SOCS1, suppressor of cytokine signaling 1.

CS-exo decreased Notch2 expression in lung tissues (Fig. S7A and B). Subsequently, miR-21a-5p antagomir (anti-miR-21a-5p) or NC was administered to the mice prior to the challenge with CS-exo. miR-21a-5p inhibition decreased the percentage of M2 macrophages in BALF (Fig. 6F and G), and increased Notch2 and SOCS1 expression in lung tissues (Fig. S7C and D).

Furthermore, mice were treated with mechanical ventilation to further validate the effects of miR-21a-5p *in vivo*. C57BL/6 mice were ventilated with low (8 ml/kg) or high (30 ml/kg) tidal volumes for 2 h. As shown in Fig. 6H, the expression of miR-21a-5p in the mechanical ventilated model was significantly increased. The percentage of M2 macrophages in BALF was upregulated in both the HtVt and LtVt groups compared to the control group; however, there was no difference between high- and low-tidal volume groups, while the percentage of M1 macrophages was not significantly altered (Fig. 6I and J). Mechanical ventilation also decreased the expression of Notch2 and SOCS1 in lung tissues (Fig. S7E and F). Notably, as shown in Fig. 6K and L, the proportion of M2 macrophages was significantly decreased in mice that were treated with miR-21a-5p antagomir prior to ventilation.

In addition, miR-21a-5p agomir was used to mimic the high levels of miR-21a-5p in ventilated mice. The Notch2 and SOCS1 levels were decreased after the mice were administered miR-21a-5p agomir (Fig. S7G and H), and the proportion of M2 macrophages increased (Fig. S7I and J). However, the increase in the expression of Notch2 using its ligand, JAG,

reversed these effects (Fig. S7G, H, K and L). In summary, these data indicated that mechanical ventilation induced the release of exosomal miR-21a-5p from epithelial cells, which can be taken up by macrophages to promote M2 macrophages via downregulating Notch2/SOCS1 (Fig. 7).

Discussion

The present study demonstrated that exosomes released by CS-treated ECs were internalized by macrophages, resulting in M2 macrophage polarization. Additionally, it was demonstrated that EC-derived exosomes contained miR-21a-5p and promoted macrophage M2 polarization via the downregulation of the Notch2/SOCS1 signaling axis in the recipient macrophages in mechanical ventilation (Fig. 7).

Intercellular communication between pulmonary ECs and macrophages maintains pulmonary homeostasis under physiological conditions (7). Macrophages are activated when homeostasis is disturbed. Previous research has emphasized the emerging role of exosomes in intercellular signal transmission and exosomes, as extracellular vesicles, can transfer RNAs, DNAs, lipids, and proteins via autocrine and paracrine mechanisms (18); this provides a medium between ECs and macrophages in lung tissue. In lung tissue, exosomes can mediate macrophage polarization through multiple pathways. Adipose-derived mesenchymal stem cell-derived exosomes promote macrophage polarization by inhibiting TLR4 and

alleviating lung injury (43). Previous studies have demonstrated that alveolar epithelial-derived exosomes also mediate macrophage activation (29,44). These results indicate that exosomes play a critical role in AM activation. The present study demonstrated that exosomes derived from alveolar ECs treated with CS were internalized by macrophages and promoted M2 polarization. CS-exo also induced the release of IL-10 in macrophages, suggesting that exosomes-derived from CS-treated ECs exerted an anti-inflammatory effect.

miRNAs are the main contents transferred in exosomes, which serve as novel regulators of cellular functions by inhibiting translation or inducing mRNA degradation. Certain miRNAs may be transferred into exosomes and delivered to target cells to regulate cell functions (45). Yao *et al* (46) demonstrated that miR-21 in mesenchymal stem cell-derived exosomes promoted M2 macrophage polarization in sepsis. In addition, Lee *et al* (47) demonstrated that miR-21 antagonism inhibited M2 macrophage polarization and reduced airway hyperresponsiveness. These findings indicated that miR-21 plays an essential role in the regulation of M2 macrophage polarization. It was also suggested that CS-treated EC-derived exosomal miR-21a-5p promoted M2 macrophage polarization, which may function as a regulator of macrophage polarization.

The specific mechanisms by which miR-21a-5p induced the polarization of macrophages remain to be further investigated. TagertScan assays were used to predict the possible targets mRNA of miR-21a-5p. When exploring miR-21a-5p protein interactions, Notch2, a highly conserved cell surface receptor, attracted our interest, as it is closely related to macrophage polarization (48-50). Notch2 is mainly expressed in stem cells and primordial cells, and also widely exists on the surface of macrophages, dendritic cells and B cells (41). Zhang *et al* (51) found that Notch2 signal transduction negatively regulated inflammatory cytokines and signal transduction in macrophages. Herein, a dual-luciferase reporter assay confirmed that miR-21a-5p could bind to the predicted binding site of Notch2. CS-exo containing miR-21a-5p decreased the expression of Notch2 mRNA and protein in macrophages. miR-21a-5p mimic transfection also decreased the protein expression of Notch2. CS-exo containing miR-21a-5p also resulted in M2 macrophage polarization. By contrast, the overexpression of Notch2 reversed these results. However, the inhibition of miR-21a-5p prior to CS-exo treatment decreased the M2 macrophage polarization which induced by CS-exo.

Decreased Notch signaling promotes M2 macrophage polarization (50), while SOCS3 expression is selectively associated with M1 macrophages and is essential for maintaining their properties (52). In the present study, SOCS1 protein downregulation was strongly associated with M2 macrophage polarization in the CS-exo group compared to the non-CS-exo group. However, SOCS1 mRNA expression was increased in the CS-exo group. There are several reasons for the poor concordance between the level of SOCS1 mRNA and protein. First, the process of mRNA translation into protein is complex and regulated by post-transcriptional modification, which renders it impossible to compute protein concentration from mRNA; second, protein half-life may differ *in vivo* (53,54). These mechanisms are ubiquitous in eukaryotic cells, which may lead to inconsistencies in the levels of SOCS1 mRNA and protein. In the present study, the Co-IP results confirmed

the interaction between SOCS1 and Notch2 in macrophages. Notch2 activation decreased the percentage of M2 macrophages, while SOCS1 downregulation (using SOSC1 siRNA) prior to Notch2 activation reversed this decrease. These findings suggested that the Notch2/SOCS1 axis affected macrophage polarization.

Finally, the present study demonstrated the role of exosomal miR-21a-5p in mechanical ventilation. CS-exo administration increased the expression level of miR-21a-5p in lung tissue and promoted M2 macrophage polarization *in vivo*, while miR-21a-5p inhibition prior to the administration of CS-exo markedly reduced M2 macrophage activation; this indicated that miR-21a-5p contributed to M2 macrophage polarization induced by CS-exo. Furthermore, mechanical ventilation for 2 h increased the expression of miR-21a-5p and the proportion of M2 macrophages in BALF. The inhibition of miR-21a-5p (using miR-21a-5p antagomir) led to the inactivation of M2 macrophages in BALF during ventilation. These results further suggested that epithelial-derived exosomes regulated M2-type macrophage polarization during short-term mechanical ventilation.

In conclusion, the presents study demonstrated that exosomes derived from mechanically stretched ECs mediated the polarization of M2 macrophages. Exosomal miR-21a-5p mediated the crosstalk between ECs and macrophages, and promoted M2 macrophage activation by inhibiting Notch2/SOCS1. The findings presented herein provide novel information about the effects of exosomal miR-21a-5p-derived from ECs on M2 macrophage polarization during mechanical ventilation, and may serve as a potential treatment strategy for VILI.

Availability of data and materials

The datasets generated and/or analyzed during the current study are available in the NCBI Gene Expression Omnibus Archive, with the accession no. GSE200932. The other raw data supporting the conclusions of the current study are available from the corresponding author on reasonable request.

Authors' contributions

YW, WX and QW designed and conceived the study. YW, YH, XL and JL performed the cell experiments and acquired the data. YX, LC, GL and YF performed the animal experiments. ZX and YW analyzed and interpreted the results. QW provided the reagents and expertise. YW and WX wrote the manuscript. YW and QW confirm the authenticity of all the

raw data. All authors have read and approved the final version of the manuscript.

Ethics approval and consent to participate

All procedures for the animal experiments were approved (approval no. 2406) by the Institutional Animal Care and Use Committee at Tongji Medical College, Huazhong University of Science and Technology (Wuhan, China).

Patient consent for publication

Not applicable

Competing interests

The authors declare that they have no competing interests.

References

1. Tremblay L, Valenza F, Ribeiro SP, Li J and Slutsky AS: Injurious ventilatory strategies increase cytokines and c- fos m-RNA expression in an isolated rat lung model. J Clin Invest 99: 944-952, 1997.
2. Ranieri VM, Suter PM, Tortorella C, De Tullio R, Dayer JM, Brienza A, Bruno F and Slutsky AS: Effect of mechanical ventilation on inflammatory mediators in patients with acute respiratory distress syndrome. JAMA 282: 54-61, 1999.
3. Imai Y, Parodo J, Kajikawa O, de Perrot M, Fischer S, Edwards V, Cutz E, Liu M, Keshavjee S, Martin TR, et al: Injurious mechanical ventilation and end-organ epithelial cell apoptosis and organ dysfunction in an experimental model of acute respiratory distress syndrome. JAMA 289: 2104-2112, 2003.
4. Silva PL, Negrini D and Macêdo Rocco PR: Mechanisms of ventilator-induced lung injury in healthy lungs. Best Pract Res Clin Anaesthesiol 29: 301-313, 2015.
5. Imanaka H, Shimaoka M, Matsuura N, Nishimura M, Ohta N and Kiyono H: Ventilator-induced lung injury is associated with neutrophil infiltration, macrophage activation, and TGF-beta 1 mRNA upregulation in rat lungs. Anesth. Analg 92: 428-436, 2001.
6. Bissonnette EY, Lauzon-Joset JF, Debley JS and Ziegler SF: Cross-talk between alveolar macrophages and lung epithelial cells is essential to maintain lung homeostasis. Front Immunol 11: 583042, 2020.
7. Guillot L, Nathan N, Tabary O, Thouvenin G, Le Rouzic P, Corvol H, Amselem S and Clement A: Alveolar epithelial cells: Master regulators of lung homeostasis. Int J Biochem Cell Biol 45: 2568-2573, 2013.
8. Opitz B, van Laak V, Eitel J and Suttorp N: Innate immune recognition in infectious and noninfectious diseases of the lung. Am J Resp Crit Care 181: 1294-1309, 2010.
9. Cheng P, Li S and Chen H: Macrophages in lung injury, repair, and fibrosis. Cells 10: 436, 2021.
10. Laskin DL, Malaviya R and Laskin JD: Role of macrophages in acute lung injury and chronic fibrosis induced by pulmonary toxicants. Toxicol Sci 168: 287-301, 2019.
11. Bhattacharya J and Westphalen K: Macrophage-epithelial interactions in pulmonary alveoli. Semin Immunopathol 38: 461-469, 2016.
12. Corvol H, Flamein F, Epaud R, Clement A and Guillot L: Lung alveolar epithelium and interstitial lung disease. Int J Biochem Cell Biol 41: 1643-1651, 2009.
13. Skerrett SJ, Liggitt HD, Hajjar AM, Ernst RK, Miller SI and Wilson CB: Respiratory epithelial cells regulate lung inflammation in response to inhaled endotoxin. Am J Physiol Lung Cell Mol Physiol 287: L143-L152, 2004.
14. Cohen TS, Cavanaugh KJ and Margulies SS: Frequency and peak stretch magnitude affect alveolar epithelial permeability. Eur Respir J 32: 854-861, 2008.
15. Heise RL, Stober V, Cheluvaraju C, Hollingsworth JW and Garantziotis S: Mechanical stretch induces epithelial-mesenchymal transition in alveolar epithelia via hyaluronan activation of innate immunity. J Biol Chem 286: 17435-17444, 2011.
16. Beckmann A, Grissmer A, Meier C and Tschernig T: Intercellular communication between alveolar epithelial cells and macrophages. Ann Anat 227: 151417-151417, 2020.
17. Mayer AK, Bartz H, Fey F, Schmidt LM and Dalpke AH: Airway epithelial cells modify immune responses by inducing an anti-inflammatory microenvironment. Eur J Immunol 38: 1689-1699, 2008.
18. Iraci N, Leonardi T, Gessler F, Vega B and Pluchino S: Focus on extracellular vesicles: Physiological role and signalling properties of extracellular membrane vesicles. Int J Mol Sci 17: 171, 2016.
19. Ambros V: The functions of animal microRNAs. Nature 431: 350-355, 2004.
20. Tomankova T, Petrek M and Kriegova E: Involvement of microRNAs in physiological and pathological processes in the lung. Respir Res 11: 159, 2010.
21. Wang T, Jiang L, Wei X, Dong Z, Liu B, Zhao J, Wang L, Xie P, Wang Y and Zhou S: Inhibition of miR-221 alleviates LPS-induced acute lung injury via inactivation of SOCS1/NF-κB signaling pathway. Cell Cycle 18: 1893-1907, 2019.
22. Li Q, Ge YL, Li M, Fang XZ, Yuan YP, Liang L and Huang SQ: miR-127 contributes to ventilator-induced lung injury. Mol Med Rep 16: 4119-4126, 2017.
23. Liu ZL, Wang H, Liu J and Wang ZX: MicroRNA-21 (miR-21) expression promotes growth, metastasis, and chemo- or radioresistance in non-small cell lung cancer cells by targeting PTEN. Mol Cell Biochem 372: 35-45, 2013.
24. da Costa Martins PA and De Windt LJ: miR-21: A miRaculous socratic paradox. Cardiovasc Res 87: 397-400, 2010.
25. Zhu WD, Xu J, Zhang M, Zhu TM, Zhang YH and Sun K: MicroRNA-21 inhibits lipopolysaccharide-induced acute lung injury by targeting nuclear factor-κB. Exp Ther Med 16: 4616-4622, 2018.
26. Ding Y, Hou Y, Liu Y, Xie X, Cui Y and Nie H: Prospects for miR-21 as a target in the treatment of lung diseases. Curr Pharm Des 27: 415-422, 2021.
27. Alipoor SD, Mortaz E, Garssen J, Movassaghi M, Mirsaeidi M and Adcock IM: Exosomes and exosomal miRNA in respiratory diseases. Mediat Inflamm 216: 5628404, 2016.
28. Jiao Y, Zhang T, Zhang C, Ji H, Tong X, Xia R, Wang W, Ma Z and Shi X: Exosomal miR-30d-5p of neutrophils induces M1 macrophage polarization and primes macrophage pyroptosis in sepsis-related acute lung injury. Crit Care 25: 356, 2021.
29. Liu F, Peng W, Chen J, Xu Z, Jiang R, Shao Q, Zhao N and Qian K: Exosomes derived from alveolar epithelial cells promote alveolar macrophage activation mediated by miR-92a-3p in sepsis-induced acute lung injury. Front Cell Infect Microbiol 11: 646546, 2021.
30. Liu Q, Xie W, Wang Y, Chen S, Han J, Wang L, Gui P and Wu Q: JAK2/STAT1-mediated HMGB1 translocation increases inflammation and cell death in a ventilator-induced lung injury model. Lab Invest 99: 1810-1821, 2019.
31. Livak KJ and Schmittgen TD: Analysis of relative gene expression data using real-time quantitative PCR and the 2(-Delta Delta C(T)) method. Methods 25: 402-408, 2001.
32. Xu H, Ling M, Xue J, Dai X, Sun Q, Chen C, Liu Y, Zhou L, Liu J, Luo F, et al: Exosomal microRNA-21 derived from bronchial epithelial cells is involved in aberrant epithelium-fibroblast cross-talk in COPD induced by cigarette smoking. Theranostics 8: 5419-5433, 2018.
33. Jiang K, Yang J, Guo S, Zhao G, Wu H and Deng G: Peripheral circulating exosome-mediated delivery of miR-155 as a novel mechanism for acute lung inflammation. Mol Ther 27: 1758-1771, 2019.
34. Li W, Qiu X, Jiang H, Han Y, Wei D and Liu J: Downregulation of miR-181a protects mice from LPS-induced acute lung injury by targeting Bcl-2. Biomed Pharmacother 84: 1375-1382, 2016.
35. Liu Q, Du J, Yu X, Xu J, Huang F, Li X, Zhang C, Li X, Chang J, Shang D, et al: miRNA-200c-3p is crucial in acute respiratory distress syndrome. Cell Discov 3: 17021, 2017.
36. Xiao J, Tang J, Chen Q, Tang D, Liu M, Luo M, Wang Y, Wang J, Zhao Z, Tang C, et al: miR-429 regulates alveolar macrophage inflammatory cytokine production and is involved in LPS-induced acute lung injury. Biochem J 471: 281-291, 2015.
37. Wynn TA, Chawla A and Pollard JW: Macrophage biology in development, homeostasis and disease. Nature 496: 445-455, 2013.
38. Murray PJ, Allen JE, Biswas SK, Fisher EA, Gilroy DW, Goerdt S, Gordon S, Hamilton JA, Ivashkiv LB, Lawrence T, et al: Macrophage activation and polarization: Nomenclature and experimental guidelines. Immunity 41: 14-20, 2014.

39. Ivashkiv LB: Epigenetic regulation of macrophage polarization and function. Trends Immunol 34: 216-223, 2013.

40. Hu G and Christman JW: Editorial: Alveolar macrophages in lung inflammation and resolution. Front Immunol 10: 2275, 2019.

41. Fortini ME: Notch signaling: The core pathway and its posttranslational regulation. Dev Cell 16: 633-647, 2009.

42. Greenbaum D, Colangelo C, Williams K and Gerstein M: Comparing protein abundance and mRNA expression levels on a genomic scale. Genome Biol 4: 117, 2003.

43. Tian J, Cui X, Sun J and Zhang J: Exosomal microRNA-16-5p from adipose mesenchymal stem cells promotes TLR4-mediated M2 macrophage polarization in septic lung injury. Int Immunopharmacol 98: 107835, 2021.

44. Chen Z, Wu H, Shi R, Fan W, Zhang J, Su W, Wang Y and Li P: miRNAomics analysis reveals the promoting effects of cigarette smoke extract-treated Beas-2B-derived exosomes on macrophage polarization. Biochem Bioph Res Co 572: 157-163, 2021.

45. He C, Zheng S, Luo Y and Wang B: Exosome theranostics: Biology and translational medicine. Theranostics 8: 237-255, 2018.

46. Yao M, Cui B, Zhang W, Ma W, Zhao G and Xing L: Exosomal miR-21 secreted by IL-1β-primed-mesenchymal stem cells induces macrophage M2 polarization and ameliorates sepsis. Life Sci 264: 118658, 2021.

47. Lee HY, Hur J, Kang JY, Rhee CK and Lee SY: MicroRNA-21 inhibition suppresses Alveolar M2 macrophages in an ovalbumin-induced allergic asthma mice model. Allergy Asthma Immunol Res 13: 312-329, 2021.

48. Kovall RA: Structures of CSL, notch and mastermind proteins: Piecing together an active transcription complex. Curr Opin Struct Biol 17: 117-127, 2007.

49. Fiúza UM and Arias AM: Cell and molecular biology of notch. J Endocrinol 194: 459-474, 2007.

50. Wang Y, He F, Feng F, Liu XW, Dong GY, Qin HY, Hu XB, Zheng MH, Liang L, Feng L, *et al*: Notch signaling determines the M1 versus M2 polarization of macrophages in antitumor immune responses. Cancer Res 70: 4840-4849, 2010.

51. Zhang Q, Wang C, Liu Z, Liu X, Han C, Cao X and Li N: Notch signal suppresses toll-like receptor-triggered inflammatory responses in macrophages by inhibiting extracellular signal-regulated kinase 1/2-mediated nuclear factor κB activation. J Biol Chem 287: 6208-6217, 2012.

52. Liu Y, Stewart KN, Bishop E, Marek CJ, Kluth DC, Rees AJ and Wilson HM: Unique expression of suppressor of cytokine signaling 3 is essential for classical macrophage activation in rodents in vitro and in vivo. J Immunol 180: 6270-6278, 2008.

53. Pascal LE, True LD, Campbell DS, Deutsch EW, Risk M, Coleman IM, Eichner LJ, Nelson PS and Liu AY: Correlation of mRNA and protein levels: Cell type-specific gene expression of cluster designation antigens in the prostate. BMC Genomics 9: 246, 2008.

54. Gygi SP, Rochon Y, Franza BR and Aebersold R: Correlation between protein and mRNA abundance in yeast. Mol Cell Biol 19: 1720-1730, 1999.